

Doping-induced band shifts and Lifshitz transitions in heavy-fermion metals

Adel Benlagra^{1,2} and Matthias Vojta²

¹*Institute for Theoretical Physics, ETH Zürich, 8093 Zürich, Switzerland*

²*Institut für Theoretische Physik, Technische Universität Dresden, 01062 Dresden, Germany*

(Dated: November 26, 2012)

For some heavy-fermion compounds, it has been suggested that a Fermi-surface-changing Lifshitz transition, which can be driven, e.g., by varying an applied magnetic field, occurs inside the heavy-fermion regime. Here we discuss, based on microscopic calculations, how the location of such a transition can be influenced by carrier doping. Due to strong correlations, a heavy band does not shift rigidly with the chemical potential. Intriguingly, we find that the actual shift is determined by the *interplay* of heavy and additional light bands crossing the Fermi level: doped carriers tend to populate heavy and light bands equally, despite the fact that the latter contribute a small density of states of excitations only. This invalidates naive estimates of the transition shift based on the low-temperature specific heat of the heavy Fermi liquid. We discuss applications of our results.

PACS numbers: 71.27.+a, 72.15.Qm, 75.20.Hr, 75.30.Mb

I. INTRODUCTION

Quantum phase transitions in metals are an active area of research.^{1,2} A large fraction of the experimentally studied cases occur in heavy-fermion metals, where strongly localized (*f*) electrons coexist with more itinerant conduction (*c*) electrons.^{3,4} Quite often, the measured deviations from Fermi-liquid behavior appear incompatible with predictions from standard quantum critical theories.^{2,5,6} At present, it is unclear whether this is related to yet unexplored types of criticality, to the influence of quenched disorder, or to the presence of non-universal energy scales preventing to reach the asymptotic critical regime. Given the smallness of the effective bandwidth of heavy fermions, which is set by the single-impurity Kondo temperature $T_K^{(1)}$, it is sometimes difficult to separate single-particle (i.e. band-structure) effects from those of collective fluctuations.

Recent experiments, utilizing both quantum oscillations and magnetotransport, aim at detecting Fermi-surface changes across quantum phase transitions, with YbRh₂Si₂,^{7,8} CeRhIn₅,^{9,10} CeRh_{1-x}Co_xIn₅,¹¹ CeRu₂Si₂,^{12,13} and URhGe¹⁴ being prominent examples. Such changes are expected for density-wave transitions where the lattice translation symmetry gets broken,^{1,2,15} for Lifshitz transitions, i.e., transitions in the topology of the Fermi surface without symmetry breaking,^{16,17} and for the more exotic Kondo-breakdown, or orbital-selective Mott, transitions, where the heavy quasiparticles themselves cease to exist.^{18–24}

A feature of standard Lifshitz transitions is that they can be easily accessed by carrier doping, which simply shifts the chemical potential, whereas they couple to pressure only indirectly (via distortions of the quasiparticle dispersion) – the latter is in contrast to expectations for both density-wave and Kondo-breakdown transitions. For YbRh₂Si₂, where a QCP is reached by applying a small magnetic field,²⁵ carrier-doping experiments were proposed in Ref. 26 in order to discriminate between

different transition scenarios: For bandstructure-related transitions, such as Lifshitz transitions, carrier doping – as opposed to isoelectronic doping or pressure – may be used to directly tune the transition field. This proposal rests on the idea that the heavy-fermion band responsible for a potential Lifshitz transition will be shifted relative to the Fermi level upon doping, while approximately preserving its shape.

This idea prompts two questions, relevant for any Lifshitz transition in heavy-fermion metals: (i) How does such a doping-induced band shift occur, given the fact that the Abrikosov-Suhl resonance (which is responsible for heavy-band formation) is quite generically pinned to the Fermi level? (ii) Can one quantitatively estimate the shift, e.g., using the amount of doping and the low-energy density of states (DOS) of Fermi-liquid excitations (obtained from the low-temperature specific heat) as input?

In this paper, we shall answer these questions through explicit microscopic calculations for the Fermi-liquid regime of heavy-fermion metals. Our findings can be summarized as follows: (a) Features of heavy-fermion bands, like band edges or van-Hove singularities, indeed shift upon varying the chemical potential, but they do so much slower than those of uncorrelated bands. More precisely, their shift is suppressed by a factor which roughly equals $Z^{-1} = m^*/m$ but also depends on further microscopic details. Here, m^* is the effective mass and Z the quasiparticle weight of the heavy carriers. (b) Since the low-energy DOS of excitations is enhanced by the same factor Z^{-1} , an estimate of the band shift via the specific-heat coefficient, $\gamma = C/T$, would be appropriate (at least approximately) *if* the heavy band under consideration would be the only band crossing the Fermi level. However, this is often not the case. (c) In the presence of both heavy-fermion and weakly correlated bands, doped carriers enter *both* types of bands roughly equally – despite the small specific-heat contribution of the weakly correlated bands – because the latter shift faster upon varying the chemical potential as compared to the heavy bands, which instead tend to be pinned to the Fermi level.

Then, the band shift *cannot* be estimated from the specific heat, but also depends on the number and properties of the uncorrelated bands.

Together, this implies that the shift of heavy-fermion bands with doping is generically slower than one would estimate from a free-particle picture, i.e., more carrier doping is required to affect the location of Lifshitz transitions. This is of potential relevance for recent experiments on Fe-doped YbRh₂Si₂.²⁷

We note that our analysis below is restricted to Lifshitz transitions well inside the heavy-fermion regime. For magnetic-field-driven transitions, this restriction conservatively implies that the transition field should be small compared to the Kondo temperature. Otherwise, the applied field leads to a sizeable polarization of the local moments. Then, a Lifshitz transition could be accompanied by a field-induced breakdown of Kondo screening, which would require a separate analysis. Interestingly, a recent numerical study²⁸ suggests that even for sizeable moment polarization accompanying heavy-fermion metamagnetism, the concept of a heavy-band Lifshitz transition remains well-defined.

The remainder of the paper is organized as follows: In Sec. II we describe the model Hamiltonian to be employed in our calculations, together with the relevant approximations. Sec. III is devoted to the behavior of a single heavy-fermion band under variations of the chemical potential. Sec. IV then describes the crucial interplay between light and heavy bands. A discussion of applications closes the paper.

II. MICROSCOPIC MODELLING

In this section, we introduce the model and method for our microscopic approach.

A. Periodic Anderson model

To describe the heavy-fermion system under the influence of doping, we employ a periodic Anderson model (PAM)³ of hybridized c and f bands,

$$\mathcal{H} = \sum_{\mathbf{k}\sigma} \left[\epsilon_{\mathbf{k}} c_{\mathbf{k}\sigma}^\dagger c_{\mathbf{k}\sigma} + \epsilon_f f_{\mathbf{k}\sigma}^\dagger f_{\mathbf{k}\sigma} + V_{\mathbf{k}} (c_{\mathbf{k}\sigma}^\dagger f_{\mathbf{k}\sigma} + \text{H.c.}) \right] + U \sum_i n_{i\downarrow}^f n_{i\uparrow}^f, \quad (1)$$

in standard notation. In what follows, the hybridization between the c and f fermion bands will be assumed to be local, $V_{\mathbf{k}} = V$, and the local Coulomb repulsion between the f -electrons will be taken to be the largest energy scale, $U \rightarrow \infty$.

The heavy Fermi-liquid phase of this model can be captured within a local self-energy approximation,

$$\Sigma_f(\mathbf{k}, \omega) \rightarrow \Sigma_f(\omega). \quad (2)$$

Being interested in qualitative low-energy properties at $T = 0$, we resort to a standard slave-boson mean-field treatment.^{3,29}

B. Slave-boson mean-field approximation

In the $U \rightarrow \infty$ limit, double occupied states for the f electrons are projected out. The remaining three states of the f orbital can be represented by spinless bosons b_i and auxiliary fermions $\tilde{f}_{i\sigma}$ with a local constraint:

$$f_{i\sigma}^\dagger \rightarrow \tilde{f}_{i\sigma}^\dagger b_i, \quad \sum_{\sigma} \tilde{f}_{i\sigma}^\dagger \tilde{f}_{i\sigma} + b_i^\dagger b_i = 1. \quad (3)$$

In the simplest saddle-point approximation, formally justified in a limit where the spin symmetry of the original model is extended from SU(2) to SU(N) with $N \rightarrow \infty$, the bosonic fields b_i are condensed, and the constraints are implemented by static Lagrange multipliers λ_i . Moreover, for a translational invariant saddle point, both fields are uniform, $b_i \equiv b$ and $\lambda_i \equiv \lambda$. The original interacting PAM is mapped onto a non-interacting two-band model with a renormalized f level energy, $\tilde{\epsilon}_f = \epsilon_f + \lambda$, and a renormalized hybridization $\tilde{V} = bV$. Diagonalization yields two dispersing bands,

$$E_{\mathbf{k}}^\pm = \frac{\epsilon_{\mathbf{k}} + \tilde{\epsilon}_f \pm \sqrt{(\epsilon_{\mathbf{k}} - \tilde{\epsilon}_f)^2 + 4\tilde{V}^2}}{2}, \quad (4)$$

describing sharp quasiparticles formed as a mixture of f and c degrees of freedom. This approximation corresponds to a purely real f -electron self energy

$$\Sigma_f(\omega) = \lambda b^{-2} + (1 - b^{-2})(\omega - \epsilon_f). \quad (5)$$

such that b is also a measure of the mass renormalization and weight of the quasiparticles, $m/m^* = Z = b^2$. A low-temperature Kondo (or coherence) scale may be defined via $T_{\text{coh}} = b^2 W$ where W is the half-bandwidth of the conduction band.

The parameters λ and b are obtained from the mean-field equations

$$V \sum_{\mathbf{k}\sigma} \langle \tilde{f}_{\mathbf{k}\sigma}^\dagger c_{\mathbf{k}\sigma} + \text{h.c.} \rangle = -2\mathcal{N}\lambda b, \quad (6a)$$

$$\sum_{\mathbf{k}\sigma} \langle \tilde{f}_{\mathbf{k}\sigma}^\dagger \tilde{f}_{\mathbf{k}\sigma} \rangle = \mathcal{N}(1 - b^2) \quad (6b)$$

where \mathcal{N} is the number of lattice sites.

Detailed numerical studies using dynamical mean-field theory^{30,31} and its cluster generalizations³² have verified that the effective two-band picture emerging from the slave-boson approximation qualitatively captures the low-energy physics of the heavy Fermi-liquid phase of the PAM.

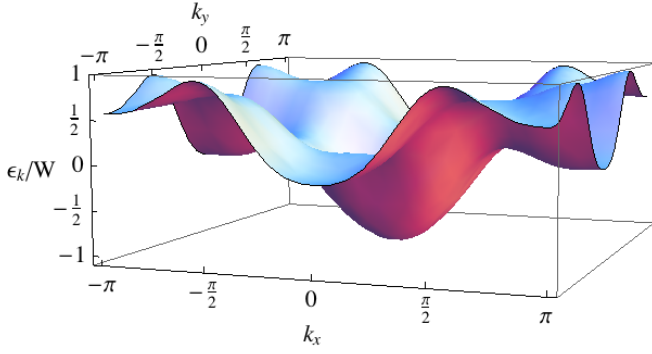


FIG. 1: The bare band dispersion $\epsilon_{\mathbf{k}}$ as defined in Eq. (7) in the first Brillouin zone. Notice the weakly dispersing piece near $\mathbf{k} = (\pi, 0)$ and $(0, \pi)$.

C. Band structure

As we are interested in Lifshitz transitions well inside the heavy-fermion regime, we study a situation with a shallow Fermi pocket within the heavy-fermion band. We generate this simply by “engineering” the bare conduction-electron band $\epsilon_{\mathbf{k}}$ such that it has a weakly dispersing portion with local minima and maxima in the middle of the band. Specifically, we employ a dispersion on a 2d square lattice which includes longer-range hopping terms:

$$\begin{aligned} \epsilon_{\mathbf{k}} = & -2t_{10}(\cos k_x + \cos k_y) - 2t_{20}(\cos 2k_x + \cos 2k_y) \\ & - 2t_{40}(\cos 4k_x + \cos 4k_y) - 4t_{11} \cos k_x \cos k_y \\ & - 4t_{22} \cos 2k_x \cos 2k_y - 4t_{33} \cos 3k_x \cos 3k_y - t_{00}, \end{aligned} \quad (7)$$

with parameters $t_{10} = 2t_{20} = 2.04 \times 10^{-1}$, $t_{40} = -2.92 \times 10^{-2}$, $t_{11} = 1.02 \times 10^{-2}$, $t_{22} = 3.40 \times 10^{-2}$, $t_{33} = 6.80 \times 10^{-3}$ and $t_{00} = 2.45 \times 10^{-1}$, which has a weakly dispersing piece near $\mathbf{k} = (\pi, 0)$ and $(0, \pi)$, as can be seen in Fig. 1. The dispersion’s half-bandwidth is $W = 1$ which we choose as our energy unit.

In the low-temperature heavy-fermion regime, the shape of the bare c band (7) will generate portions of heavy bands which disperse weakly on the scale T_{coh} . Those can be brought near the Fermi level by choosing an appropriate value of the chemical potential μ .

An example, with a heavy-fermion band structure derived from the slave-boson approximation, is shown in Fig. 2a. The weakly dispersing piece, Fig. 2b, induces a pronounced peak in the DOS at the Fermi level, on top of the usual Kondo peak originating from the Abrikosov-Suhl resonance. (Recall that the width of the latter is roughly given by WZ , here 10^{-2} .) In fact, the maximum DOS arises from the van-Hove singularity (vHs) at $\mathbf{k} = (\pi, 0)$, $(0, \pi)$ in the bare dispersion (7); this vHs is inherited by both the upper and lower renormalized bands. Together with the dispersion minimum at $\mathbf{k} = (2.75, 0)$ this defines a small and shallow Fermi pocket. Its depth

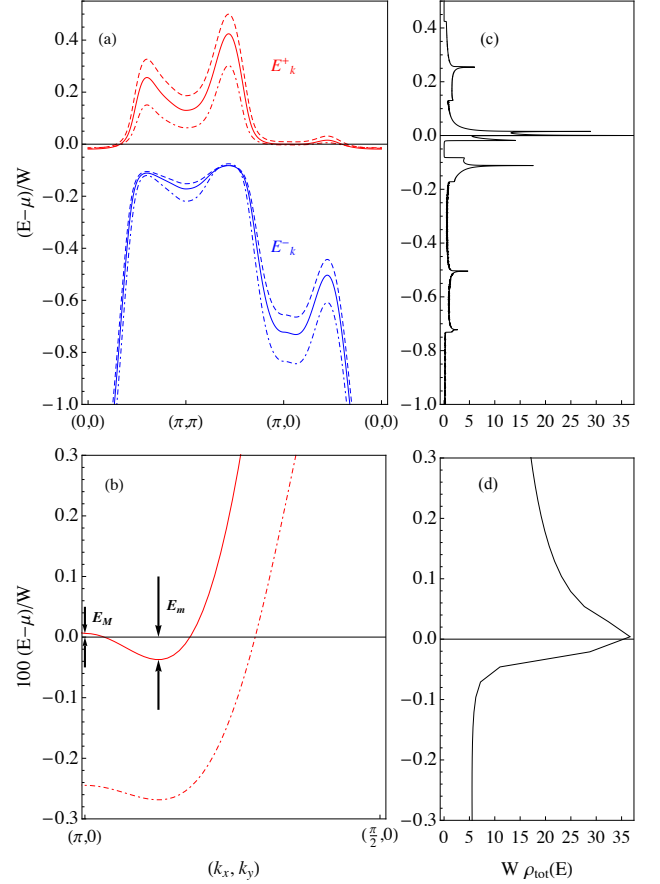


FIG. 2: (a,b): Zero-temperature heavy-fermion band structure with a shallow pocket, as obtained within the slave-boson mean-field approach. (a) shows the full dispersion of the two hybridized bands along a path in the 2d Brillouin zone for different values of the chemical potential μ , (b) a zoom near the Fermi level. The depth of the shallow Fermi pocket is $E_m \equiv E_{\mathbf{k}=(2.75,0)}^+$ whose doping evolution will be discussed in the paper. The height of the pocket defines a second scale $E_M \equiv E_{\mathbf{k}=(\pi,0)}^+$; the vHs at $(\pi, 0)$, $(0, \pi)$ produces a peak in the DOS. (c,d): Corresponding total DOS (per spin) of quasiparticles, $\rho_{\text{tot}} = \rho_c + \rho_f$. The bare band dispersion is as specified in Eq. (7), furthermore $\epsilon_f/W = -9.65$, $\mu/W = 0.575$ (resp. $\mu/W = 0.499$ for the dashed dispersion and $\mu/W = 0.651$ for the dot-dashed one) and $V/W = 1.5$, which results in a filling of $n_{\text{tot}} = 2.33$ (resp. $n_{\text{tot}} = 2.23$ and $n_{\text{tot}} = 2.45$) and a quasiparticle renormalization of $1/Z \simeq 99$ (resp. $1/Z \simeq 86$ and $1/Z \simeq 120$). Momentum integrals were performed with 1600^2 \mathbf{k} points, and a Lorentzian broadening of $10^{-5}W$ was employed for the DOS – this smears the logarithmic divergence of the DOS at the vHs.

and height are measured by E_m and E_M , respectively, see Fig. 2b.

Moving the chemical potential away from the position corresponding to Fig. 2b is expected to lead to Lifshitz transitions within the heavy-fermion regime; in particular, $E_m(\mu) = 0$ corresponds to the point where the shallow pocket disappears. Alternatively, this transition is

expected to be driven for a single spin species at finite E_m by applying a Zeeman field.

III. CARRIER DOPING OF HEAVY-FERMION BANDS

Our main objective is to understand the behavior of heavy-fermion bands upon carrier doping. We shall therefore study the PAM of Sec. II under variation of the chemical potential. Specifically, we are interested in a regime where a narrow-band feature is located near the Fermi level, and we would like to understand how a shallow Fermi pocket, as in Fig. 2b, evolves upon doping. For this purpose, we will monitor the pocket depth E_m upon doping.

We note that a variation of the chemical potential will in general have two different effects: It will cause a change in the occupation numbers and thus a band shift, but it will also cause a change in the Kondo temperature T_K . The latter effect is primarily determined by the energy dependence of the *bare* c -electron density of states at the Fermi level and therefore disconnected from the physics of the shallow bands in the *renormalized* band structure. However, a consistent calculation requires to account for both effects, because a change in T_K comes with a change in b and, via Eq. (3), a change in the f electron occupation.

A. Quantifying band shifts

In order to quantify the band-shift phenomenology, let us consider uncorrelated electrons as a reference. Here, a change in the chemical potential, $\Delta\mu$, produces a rigid band shift, such that $\Delta E_m = \Delta\mu$. Moreover, this band shift leads to a change in the occupation number n according to $\Delta n = 2\rho(0)\Delta\mu$ at zero temperature where $\rho(0)$ is the DOS (per spin) at the Fermi level. (Note that $\Delta n/\Delta\mu$ is the electronic compressibility.) For heavy Fermi liquids, this suggests to focus on the quantities

$$P = \frac{\Delta E_m}{\Delta\mu}, \quad Q = \frac{\Delta n_{\text{tot}}}{2\rho_{\text{tot}}\Delta\mu}, \quad (8)$$

where n_{tot} is the number of electrons in both the c and f bands of the model (1), and ρ_{tot} denotes the (renormalized) total DOS per spin, which is related to the $T \rightarrow 0$ specific-heat coefficient γ by the Fermi-liquid relation $\gamma = (2\pi^2/3)\rho_{\text{tot}}$. Thus the ratio

$$\frac{P}{Q} = \frac{3}{\pi^2} \frac{\Delta E_m \gamma}{\Delta n_{\text{tot}}} \quad (9)$$

relates the experimentally accessible observables Δn_{tot} and γ to the band shift ΔE_m , which itself would, e.g., correspond to a shift in the transition field of a Zeeman-induced Lifshitz transition associated with the Fermi pocket.

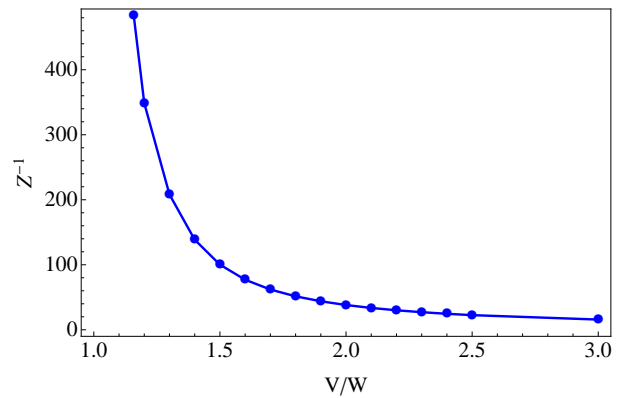


FIG. 3: Evolution of the mass renormalization $Z^{-1} = m^*/m$ with the hybridization V , as obtained from the slave-boson approximation. Here, $\epsilon_f/W = -9.65$ is kept fixed and μ is adjusted to $\mu_0(V)$ such that $|E_m| = |E_M|$, see text for details. $Z(V)$ is dominated by the exponential dependence³ of the single-impurity Kondo temperature $T_K^{(1)}$ on V .

While both P and Q equal unity for uncorrelated bands, we will show below that both quantities are suppressed by roughly $Z = m/m^*$ in the heavy-fermion regime. In the effective two-band description, the central effect which causes a deviation from the rigid-band picture is that the f occupation remains (approximately) fixed (as a result of strong correlations) upon varying the chemical potential.

For the evaluation of Q we note that, in the slave-boson approximation, the renormalized total DOS, determining the specific-heat coefficient, is simply given by the total quasiparticle DOS, $\rho_{\text{tot}} = \rho_c + \rho_{\tilde{f}}$.

B. Slave-boson results

We now turn to our numerical results from the slave-boson mean-field approximation, using the bare c band structure as described in Sec. II C. A variation of the Kondo temperature (or mass renormalization) is achieved by fixing the bare f level energy ϵ_f while varying the hybridization strength V . For each parameter set, the chemical potential μ is adjusted to a value $\mu_0(V)$ such that the Fermi pocket around $\mathbf{k} = (2.75, 0)$ is present in the upper band $E_{\mathbf{k}}^+$, with $|E_m| = |E_M|$. This prescription leads to band fillings $n_{\text{tot}} > 2$ which vary with V , but guarantees that the narrow band feature of interest is centered at the Fermi level. (Alternative choices for $\mu_0(V)$ do not alter the qualitative results.)

Fig. 3 shows the evolution of $1/Z = m^*/m$ with V where $\mu = \mu_0(V)$ for all V . As expected, $1/Z$ strongly increases upon decreasing V – this mainly reflects the exponential dependence of the Kondo temperature on V : $\ln T_K^{(1)} \propto V^2/(\epsilon_f W)$.

Fig. 4a illustrates the variation of the band filling in the vicinity of $\mu = \mu_0(V)$ for fixed $V/W = 1.5$. In Fig. 4b we show E_m , the position of the bottom of the Fermi pocket.

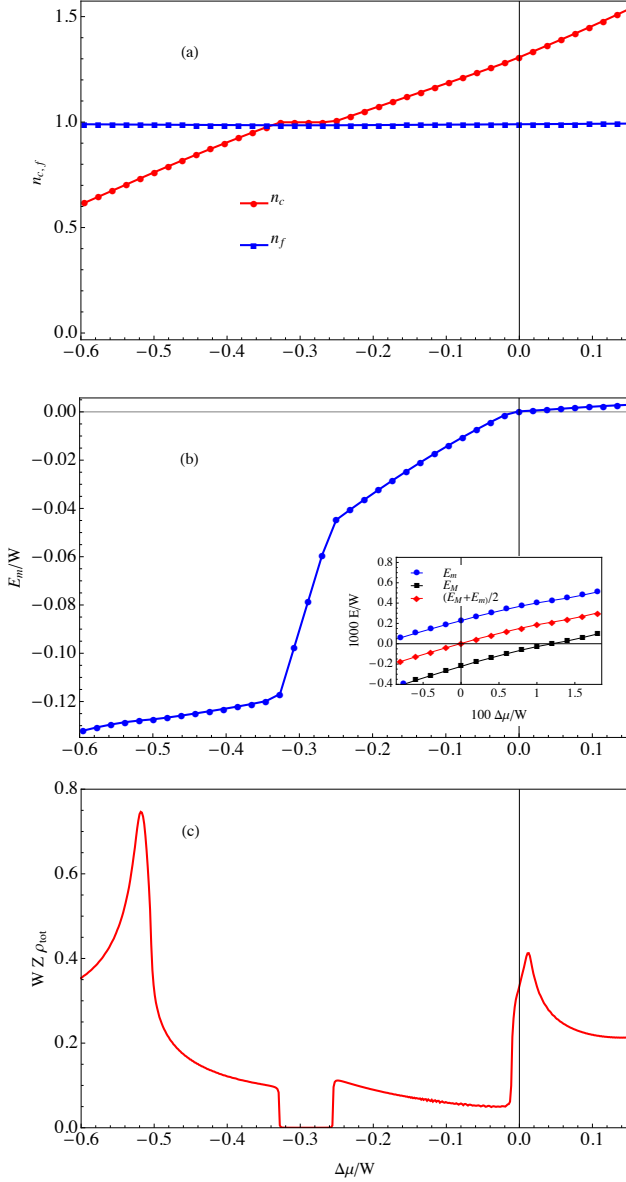


FIG. 4: Slave-boson results for (a) the band fillings $\langle n_c \rangle$ and $\langle n_f \rangle$, (b) the energy scale E_m measuring the pocket depth, and (c) the total quasiparticle DOS at the Fermi level normalized by the quasiparticle weight, $\rho_{\text{tot}}(0)Z$, as function of the chemical potential, defined via $\mu = \mu_0(V) + \Delta\mu$, where $|E_m| = |E_M|$ for $\Delta\mu = 0$. Here, $\epsilon_f/W = -9.65$, $V/W = 1.5$ are kept fixed, and $\mu_0(V)/W \simeq 0.569$. The interval $-0.33 < \Delta\mu/W < -0.26$ where $\langle n_c \rangle$, $\langle n_f \rangle$ are constant corresponds to the Kondo insulator. Comparing panel (c) with the energy-dependent DOS at *fixed* $\mu = \mu_0(V)$ in Fig. 2d illustrates again that a rigid-band picture is by no means appropriate.

It is clear that this does not follow the imposed chemical-potential variation, but changes more slowly, i.e., $P \ll 1$. As can be seen in the inset, E_m and E_M have roughly the same variation in the vicinity of $\mu_0(V)$, such that the width of the shallow Fermi pocket is approximately preserved for this range of chemical potential. Fig. 4c

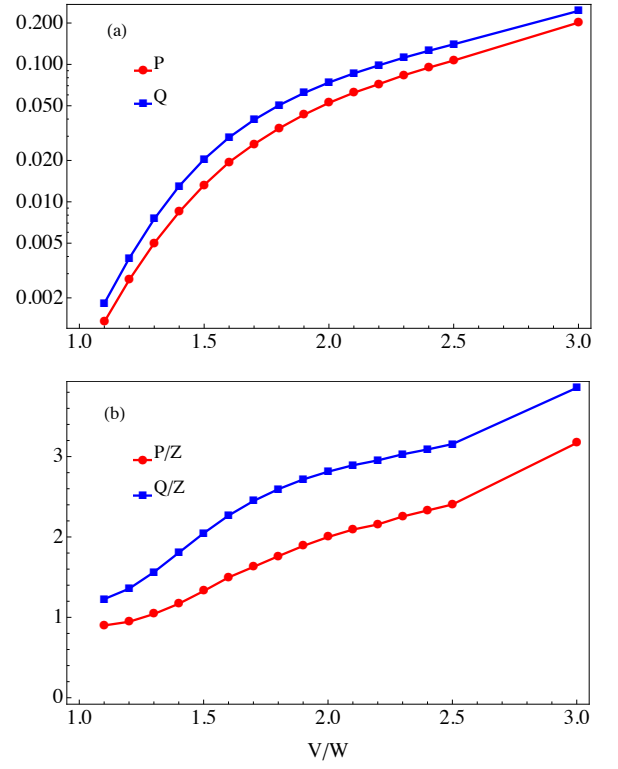


FIG. 5: (a) Dimensionless parameters P and Q , defined in Eq. (8), as function of the hybridization V , with $\epsilon_f/W = -9.65$ and $\mu = \mu_0(V)$ as before. P and Q characterize the changes of E_m and $\langle n \rangle$ with μ , respectively, and appear strongly suppressed w.r.t. the non-interacting reference value 1. (b) Re-scaled parameters P/Z and Q/Z , which are now of order unity.

also shows the evolution of the renormalized total DOS at the Fermi level. Most importantly, this DOS is large in units of $(1/W)$, such that it becomes of order unity upon multiplying by the quasiparticle residue, $WZ\rho_{\text{tot}}(0) \sim 1$. Considering the variation of the filling in Fig. 4a where $\Delta n \sim \Delta\mu/W$, it is clear that $Q/Z \sim 1$, i.e., $Q \ll 1$. Results similar to that in Fig. 4 can be found for any V .

In Fig. 5, we have collected data for P and Q obtained upon varying V . Both P and Q have been evaluated utilizing small variations of μ in the vicinity of $\mu = \mu_0(V)$.

C. Summary

For the simple two-band heavy fermion system, we have investigated the quantities P and Q , measuring the shift of heavy-band features and the change in carrier density normalized to the DOS of excitations, respectively, upon changing the chemical potential. Both P and Q , which equal unity for uncorrelated bands, are renormalized downwards by approximately a factor of $Z = m/m^*$ – this is a natural consequence of the “pinning” of the Kondo resonance (and with it the heavy band) to the Fermi level.

Interestingly, the fact that P and Q are renormalized in parallel implies that the ratio P/Q (9) is of order unity, Fig. 5b. However, as we show in the next section, this state of affairs changes once the complexity of real heavy-fermion band structures is accounted for.

IV. INTERPLAY OF LIGHT AND HEAVY BANDS

If a heavy-fermion system displays, in addition to the heavy-electron band discussed so far, other weakly correlated (i.e. light) bands crossing the Fermi level, then the quantity Q needs to be re-defined:

$$Q = \frac{\Delta n_{\text{tot,h}} + \Delta n_l}{2(\rho_{\text{tot,h}} + \rho_l)\Delta\mu} \quad (10)$$

where the indices l and h refer to the contributions from the light and heavy bands, respectively (where the “heavy” piece includes the two renormalized bands of the PAM as described in Sec. II C, with one of them crossing the Fermi level). Provided that $\rho_{\text{tot,h}} \gg \rho_l$ and using $\Delta n_l = 2\rho_l\Delta\mu$ the above equation reduces to

$$Q = \frac{\Delta n_{\text{tot,h}}}{2\rho_{\text{tot,h}}\Delta\mu} + \frac{\rho_l}{\rho_{\text{tot,h}}} = Q_h + \frac{\rho_l}{\rho_{\text{tot,h}}} \quad (11)$$

where $Q_h \sim Z$ is the heavy-band Q calculated in Sec. III. Assuming the bare DOS in a light band to be comparable to that of the c band forming the heavy fermions, we have $\rho_l/\rho_{\text{tot,h}} \sim Z$, such that both contributions in Eq. (11) are of the same order of magnitude. Moreover, ρ_l scales with the number of light bands crossing the Fermi level.

This implies that the contribution to Q , i.e., to the number of doped carriers, from the light bands is *not* negligible, despite the light bands’ DOS being much smaller than that of the heavy band. Inserting numbers, we find that P/Q can easily reach values down to 0.1–0.2, see Fig. 6, with small values occurring if the weakly correlated bands happen to have a larger DOS than the bare heavy-fermion c band. Thus, for a given number of doped carriers, the heavy-band features such as band edges and vHs shift much slower than estimated via the specific heat, the main reason being that the carriers enter both heavy and light bands simultaneously, because the light uncorrelated bands are more susceptible to changes in the chemical potential.

V. CONCLUSIONS

We have investigated the effect of carrier doping on quasiparticle bands of heavy Fermi liquids, with the goal of quantifying the shift of band-structure features such as band edges and van-Hove singularities (of shallow pockets) with doping.

We have found, not unexpectedly, that a rigid shift of heavy-fermion bands does not occur, due to the pinning

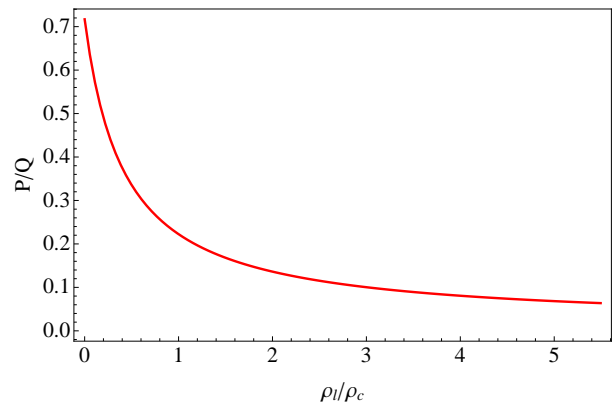


FIG. 6: Evolution of the ratio P/Q , defined in Eq. (9), with the addition of an increasing number of light bands according to Eq. (10). ρ_l scales with the number of light bands crossing the Fermi level. The heavy-band parameters are the same as in Fig. 5 with $V/W = 1.5$, and ρ_c refers to the c -electron part of the DOS per spin $\rho_{\text{tot,h}}$ of the two-band system described by the PAM with the same heavy-fermion band parameters.

of the Abrikosov-Suhl resonance to the Fermi level. This reduced band shift is paralleled by a reduced compressibility: The charge doped into a two-band heavy Fermi liquid, as described by the standard periodic Anderson model, is much smaller than its large DOS of Fermi-liquid excitations would suggest. Interestingly, these two effects tend to cancel when it comes to estimating the band shift from the doped charge via the specific-heat coefficient, Eq. (9).

For real materials another issue comes into play: Because of the reduced compressibility of the heavy bands, additional weakly correlated (i.e. light) bands cannot be neglected for the doping process, despite their small contribution to the specific heat. As a result, doped carriers populate both heavy and light bands, such that knowledge of the specific heat is not sufficient to estimate the band shift.

We now briefly discuss the application of our results to YbRh_2Si_2 . Here, recent carrier-doping experiments using Fe substituting for Rh indicate that the transition field B^* , as marked by the termination of the so-called T^* line at $T = 0$, (Refs. 7,8,33) can be tuned by doping. On the one hand, one can estimate the shift of band-structure features in a free-electron model where $P = Q = 1$. Using an approximate $\gamma = 2 \text{ J/mol K}^2$ yields a shift of $\Delta E_m = 0.06 \text{ meV}$ for 5% Fe doping. On the other hand, B^* has moved by 30 mT for this doping.²⁷ Using the high-field g factor of 3.6 this converts into $\Delta E_m = 0.006 \text{ meV}$. Therefore, if the transition is driven by band-structure features, consistency requires $P/Q \approx 0.1$. While this small value could be due to an unexpectedly large DOS of the weakly correlated bands, it is more likely that non-local correlation effects not captured in the present calculation become relevant. One candidate is a low-temperature enhancement of the g factor due to incipient ferromagnetism³⁴ – this would then

imply larger ΔE_m and hence larger P/Q . Further experiments using different dopants may shed light onto this issue: For a transition driven by band-structure effects, one would expect a shift of B^* which, to leading order, depends on the number of doped carriers only, i.e., Fe and Ru doping should have a similar effect on B^* .

Acknowledgments

The authors acknowledge fruitful discussions with F. Assaad, M. Brando, S. Friedemann, P. Gegenwart, and

Y. Tokiwa. This research has been supported by the DFG through GRK 1621 and FOR 960.

-
- ¹ S. Sachdev, *Quantum Phase Transitions*, 2nd ed., Cambridge University Press, Cambridge (2011).
 - ² H. von Löhneysen, A. Rosch, M. Vojta, and P. Wölfle, *Rev. Mod. Phys.* **79**, 1015 (2007).
 - ³ A. C. Hewson, *The Kondo Problem to Heavy Fermions*, Cambridge University Press, Cambridge (1997).
 - ⁴ P. Coleman, in: *Handbook of Magnetism and Advanced Magnetic Materials* (eds H. Kronmüller and S. Parkin), vol. 1, p. 45, Wileys, New York (2007).
 - ⁵ G. R. Stewart, *Rev. Mod. Phys.* **73**, 797 (2001).
 - ⁶ Q. Si and F. Steglich, *Science* **329**, 1161 (2010).
 - ⁷ S. Paschen, T. Lühmann, S. Wirth, P. Gegenwart, O. Trovarelli, C. Geibel, F. Steglich, P. Coleman, and Q. Si, *Nature* **432**, 881 (2004).
 - ⁸ S. Friedemann, N. Oeschler, S. Wirth, C. Krellner, C. Geibel, F. Steglich, S. Paschen, S. Kirchner, and Q. Si, *PNAS* **107**, 14547 (2010).
 - ⁹ H. Shishido, R. Settai, H. Harima, and Y. Onuki, *J. Phys. Soc. Jpn.* **74**, 1103 (2005).
 - ¹⁰ Y. Onuki and R. Settai, *Low Temp. Phys.* **38**, 89 (2012).
 - ¹¹ S. K. Goh, J. Paglione, M. Sutherland, E. C. T. O'Farrell, C. Bergemann, T. A. Sayles, and M. B. Maple, *Phys. Rev. Lett.* **101**, 056402 (2008).
 - ¹² R. Daou, C. Bergemann, and S. R. Julian, *Phys. Rev. Lett.* **96**, 026401 (2006).
 - ¹³ H. Pfau, R. Daou, M. Brando, and F. Steglich, *Phys. Rev. B* **85**, 035127 (2012).
 - ¹⁴ E. A. Yelland, J. M. Barraclough, W. Wang, K. V. Kamenev, and A. D. Huxley, *Nature Phys.* **7**, 890 (2011).
 - ¹⁵ Ya. B. Bazaliy, R. Ramazashvili, Q. Si, and M. R. Norman, *Phys. Rev. B* **69**, 144423 (2004).
 - ¹⁶ I. M. Lifshitz, *Sov. Phys. JETP* **11**, 1130 (1960).
 - ¹⁷ Y. Yamaji, T. Misawa, and M. Imada, *J. Phys. Soc. Jpn.* **75**, 094719 (2006).
 - ¹⁸ P. Coleman, C. Pépin, Q. Si, and R. Ramazashvili, *J. Phys.: Condens. Matt.* **13**, R723 (2001).
 - ¹⁹ Q. Si, S. Rabello, K. Ingersent, and J. L. Smith, *Nature (London)* **413**, 804 (2001).
 - ²⁰ T. Senthil, S. Sachdev, and M. Vojta, *Phys. Rev. Lett.* **90**, 216403 (2003).
 - ²¹ I. Paul, C. Pépin, and M. R. Norman, *Phys. Rev. Lett.* **98**, 026402 (2007).
 - ²² M. Vojta, *J. Low Temp. Phys.* **161**, 203 (2010).
 - ²³ C. Pépin, *Phys. Rev. Lett.* **98**, 206401 (2007).
 - ²⁴ We note that heavy-fermion Lifshitz transitions may occur generically near Kondo-breakdown transitions, see: A. Hackl and M. Vojta, *Phys. Rev. B* **77**, 134439 (2008).
 - ²⁵ P. Gegenwart, J. Custers, C. Geibel, K. Neumaier, T. Tayama, K. Tenya, O. Trovarelli, and F. Steglich, *Phys. Rev. Lett.* **89**, 056402 (2002).
 - ²⁶ A. Hackl and M. Vojta, *Phys. Rev. Lett.* **106**, 137002 (2011).
 - ²⁷ Y. Tokiwa, P. Gegenwart *et al.*, to be published.
 - ²⁸ M. Bercx and F. F. Assaad, *Phys. Rev. B* **86**, 075108 (2012).
 - ²⁹ P. Coleman, *Phys. Rev. B* **29**, 3035 (1984).
 - ³⁰ C. Grenzbach, F. B. Anders, G. Czycholl, and T. Pruschke, *Phys. Rev. B* **74**, 195119 (2006).
 - ³¹ K. S. D. Beach and F. F. Assaad, *Phys. Rev. B* **77**, 205123 (2008).
 - ³² L. C. Martin and F. F. Assaad, *Phys. Rev. Lett.* **101**, 066404 (2008); L. C. Martin, M. Bercx, and F. F. Assaad, *Phys. Rev. B* **82**, 245105 (2010).
 - ³³ P. Gegenwart, T. Westerkamp, C. Krellner, Y. Tokiwa, S. Paschen, C. Geibel, F. Steglich, E. Abrahams, and Q. Si, *Science* **315**, 969 (2007).
 - ³⁴ P. Gegenwart, J. Custers, Y. Tokiwa, C. Geibel, and F. Steglich, *Phys. Rev. Lett.* **94**, 076402 (2005).